Correlation of 6-^{18}F-Fluoro-L-Dopa PET Uptake with Proliferation and Tumor Grade in Newly Diagnosed and Recurrent Gliomas

Barbara J. Fueger[1], Johannes Czernin[1], Timothy Cloughesy[2], Daniel H. Silverman[1], Cheri L. Geist[1], Martin A. Walter[1], Christiaan Schiepers[1], Phioanh Nghiemphu[2], Albert Lai[2], Michael E. Phelps[1], and Wei Chen[1]

[1]*Department of Molecular and Medical Pharmacology, David Geffen School of Medicine, University of California, Los Angeles, California; and* [2]*Department of Neurology, David Geffen School of Medicine, University of California, Los Angeles, California*

6-^{18}F-fluoro-L-dopa (^{18}F-FDOPA) measured with PET as a biomarker of amino acid uptake has been investigated in brain tumor imaging. The aims of the current study were to determine whether the degree of ^{18}F-FDOPA uptake in brain tumors predicted tumor grade and was associated with tumor proliferative activity in newly diagnosed and recurrent gliomas. **Methods:** Fifty-nine patients (40 men, 19 women; mean age ± SD, 44.4 ± 12.3 y) with newly diagnosed (n = 22) or recurrent (n = 37) gliomas underwent ^{18}F-FDOPA PET perioperatively. Tumor tissue was obtained by resection or biopsy in all patients. The tumor grade and Ki-67 proliferation index were obtained by standard pathology assays. Tumor ^{18}F-FDOPA uptake was quantified by determining various standardized uptake value (SUV) parameters (mean SUV, maximum SUV [SUVmax], mean values of voxels with top 20% SUVs, and tumor–to–normal-brain tissue ratios) that were then correlated with histopathologic grade and Ki-67 proliferation index. **Results:** Fifty-nine lesions in 59 patients were analyzed. ^{18}F-FDOPA uptake was significantly higher in high-grade than in low-grade tumors for newly diagnosed tumors (SUVmax, 4.22 ± 1.30 vs. 2.34 ± 1.35, P = 0.005) but not for recurrent tumors that had gone through treatment previously (SUVmax, 3.36 ± 1.26 vs. 2.67 ± 1.18, P = 0.22). An SUVmax threshold of 2.72 differentiated low-grade from high-grade tumors, with a sensitivity and specificity of 85% and 89%, respectively, using receiver-operating-characteristic curve analysis (area under the curve, 0.86). ^{18}F-FDOPA PET uptake correlated significantly with Ki-67 tumor proliferation index in newly diagnosed tumors (r = 0.66, P = 0.001) but not in recurrent tumors (r = 0.14, P = 0.41). **Conclusion:** ^{18}F-FDOPA uptake is significantly higher in high-grade than in low-grade tumors in newly diagnosed but not recurrent tumors that had been treated previously. A significant correlation between ^{18}F-FDOPA uptake and tumor proliferation in newly diagnosed tumors was observed, whereas this correlation was not identified for recurrent tumors. Thus, ^{18}F-FDOPA PET might serve as a noninvasive marker of tumor grading and might provide a useful surrogate of tumor proliferative activity in newly diagnosed gliomas.

Received Apr. 29, 2010; revision accepted Jun. 29, 2010.
For correspondence or reprints contact: Wei Chen, 200 MP, B114-61, David Geffen School of Medicine, University of California Los Angeles, Los Angeles, CA 90095.
E-mail: weichen@mednet.ucla.edu
Guest Editor: Wolf-Dieter Heiss, Max-Planck-Institut für Neurologische Forshung

Key Words: ^{18}F-FDOPA; PET; brain tumors; tumor grade; Ki-67 proliferation index

J Nucl Med 2010; 51:1532–1538
DOI: 10.2967/jnumed.110.078592

In primary brain gliomas, markers of proliferative potential and tumor grade determined by pathologic examination of tumor tissue specimens have been among the best-established correlates of clinical outcome (*1–4*). However, gliomas are notoriously heterogeneous. Tumor tissue is often sampled by stereotactic biopsy, which may not be an accurate representation of the true malignant potential of the tumor. This might lead to a misclassification of true tumor grade and, thus, an inaccurate reflection of prognosis (*5*). Various noninvasive imaging markers have been studied in brain tumors to evaluate their predictive power in determining tumor grade and proliferative potential.

Amino acid analogs (*6–12*) and proliferation markers such as 3′-deoxy-3′-^{18}F-fluorothymidine (^{18}F-FLT) (*13–17*) have been studied for brain tumor imaging. Correlations between tumor proliferation by Ki-67 and ^{18}F-FLT uptake have been reported for ^{18}F-FLT (*14–16*) and ^{11}C-methionine (*14,18–20*). ^{18}F-labeled amino acid analogs have the advantage of easy clinical application because of the longer half-life of the ^{18}F PET tracer. It has been shown previously that the amino acid analog 6-^{18}F-fluoro-L-dopa (^{18}F-FDOPA) provides excellent visualization of high-grade and low-grade brain tumors (*21–26*). ^{18}F-FDOPA is brought into tumor cells via amino acid transporters. However, previous studies have provided conflicting data as to whether ^{18}F-FDOPA uptake differs significantly among high- and low-grade gliomas (*22,23,26*). Furthermore, it is unknown whether tumor ^{18}F-FDOPA uptake correlates with tumor proliferative activity as measured by antibody staining of the Ki-67 antigen of tumor cells.

The aims of this study were, therefore, 3-fold: first, to determine whether the degree of ^{18}F-FDOPA uptake correlated with World Health Organization (WHO) histopathologic tumor grade by pathologic verification; second, to examine whether ^{18}F-FDOPA tumor uptake and tumor cell prolifera-

tion as determined by Ki-67 index were correlated; and third, to compare these characteristics among newly diagnosed and recurrent tumors.

MATERIALS AND METHODS

Patients

The study population consisted of 17 prospectively and 42 retrospectively enrolled patients with malignant brain tumors (Table 1). There were 40 men and 19 women, with a mean age of 44 ± 12 y, ranging from 23 to 71 y. Twenty-two patients had newly diagnosed tumors and 37 patients presented with recurrent tumors who had received treatment previously. Among these 37 patients, all had gone through surgical resection. In addition to surgery, 32 patients had received chemotherapy or radiation (86%), whereas 27 patients had undergone radiation only (73%). The median time from completion of radiation to the PET scan was 51 wk. The time between ^{18}F-FDOPA PET and histologic diagnosis averaged 4.8 ± 4.2 wk (4.0 ± 4.6 wk for newly diagnosed and 5.3 ± 3.9 wk for recurrent tumors).

All prospectively enrolled patients provided written informed consent for participating in this study, which was approved by the University of California, Los Angeles, Office for Protection of Research Subjects. The consent requirements were waived by that office for the retrospectively enrolled patients who had undergone clinical ^{18}F-FDOPA PET or PET/CT scans.

PET

PET was performed on a dedicated system (ECAT HR or HR$^+$; Siemens) (*27,28*) for 49 patients, and 10 patients were imaged with a dual-detector PET/CT system (Biograph Duo; Siemens). The dedicated PET systems are equipped with bismuth germinate crystal detectors, and the PET/CT system consists of lutetium oxyorthosilicate crystal detectors and a dual-detector helical CT scanner. Our phantom study showed that differences in activity in the volumes of interest between the scanners were not significantly different from differences measured in volumes of interest within a scanner (mean difference of 2.5% in each case).

Patients were asked to fast for at least 4 h before image acquisition. ^{18}F-FDOPA was synthesized according to a previously reported procedure (*29,30*) and was injected intravenously at a dose of 1.1–6.6 MBq/kg.

For dedicated PET, data were acquired in 3-dimensional mode. Attenuation correction was calculated as reported previously (*31*). For PET/CT, a CT scan (120 kV, 80 mAs, 1-s tube rotation, 3-mm slice collimation) was acquired first. The CT data were used for attenuation correction as reported previously (*32*). For both PET and PET/CT scans, the emission scan was started 10 min after tracer injection. Images were acquired for 30 min in 3-dimensional mode. Image data acquired between 10 and 30 min were summed to obtain a 20-min static image. This time window was based on our previous experience that the highest tracer uptake in the tumor generally occurs between 10 and 30 min after ^{18}F-FDOPA injection (*23*). PET images were reconstructed using iterative techniques with ordered-subset expectation maximization consisting of 6 iterations with 8 subsets (*33*). A gaussian filter with a full width at half maximum of 4 mm was applied.

Image Analysis

Images were first inspected visually. Then the axial PET image slice displaying the maximum tumor ^{18}F-FDOPA uptake was selected. The activity counts from the 2 adjacent axial slices (1 plane above and 1 below the chosen slice) were summed to improve count statistics.

TABLE 1. Patient Characteristics

Characteristic	All patients (n = 59)	Newly diagnosed (n = 22)	Recurrent (n = 37)
Sex			
Female	19 (32)	9 (41)	10 (27)
Male	40 (68)	13 (59)	27 (73)
Age (y)			
Median	44.5	42.1	45.9
Range	23.1–71.2	23.9–64.3	23.1–71.2
Duration of disease (wk)			
Median	110.5	9.8	167.7
Range	0.1–984.69	0.1–33.4	3.9–984.9
Pathohistology			
WHO grade II	13 (22)	9 (41)	4 (11)
Astrocytoma	4 (7)	4 (18)	0
Oligoastrocytoma	3 (5)	2 (9)	1 (3)
Oligodendroglioma	6 (10)	3 (14)	3 (8)
WHO grade III	19 (32)	7 (32)	12 (32)
Anaplastic astrocytoma	8 (14)	2 (9)	6 (16)
Anaplastic oligoastrocytoma	6 (10)	3 (14)	3 (8)
Anaplastic oligodendroglioma	5 (8)	2 (9)	3 (8)
WHO grade IV	27 (46)	6 (27)	21 (57)
Glioblastoma	25 (42.4)	6 (27)	19 (51.4)
Gliosarcoma	2 (3.4)	0	2 (5.4)
Low-grade tumors	13 (22)	9 (41)	4 (11)
High-grade tumors	43 (73)	13 (59)	33 (89)
Astrocytomas	27 (46)	12 (55)	15 (41)
Nonastrocytomas	32 (54)	10 (45)	22 (59)

Data in parentheses are percentages.

Tumor regions of interest (ROIs) were defined on summed images in 2 ways. First, a standardized 10-mm circular region was placed over the area with the peak activity. This first ROI was used to derive maximum standardized uptake value (SUVmax) and mean standardized uptake value. To minimize operator dependence, an additional ROI was derived by an 80% peak-voxel-intensity isocontouring approach. This method provided the mean values of voxels with the top 20% SUVs. A normal reference brain region was defined by drawing an ROI involving the entire contralateral hemisphere at the level of the centrum semiovale to derive tumor-to-background ratios. The radiotracer concentration in the ROIs was normalized to the injected dose per kilogram of patient's body weight to derive the SUVs.

Histopathology and Immunohistochemistry

All excised tumors were graded using the WHO grading system (malignancy scale) for central nervous system tumors (*34*), and all were stained for Ki-67 expression. The available tissue was formalin-fixed and paraffin-embedded. These tissue blocks were recut, and serial sections of 3–4 μm were immunohistochemically labeled with the polyclonal antibody that labels the Ki-67 antigen. The immunohistochemistry was performed according to standard protocol (*35*). The number of Ki-67–positive cells among the total number of resting cells (Ki-67 labeling index) was determined. Ki-67 labeling index was determined through computerized morphometry as previously described (*36*). Only nuclei of tumor cells staining definitely brownish were considered positive. The percentage of nuclei stained with Ki-67 antibody per total number of nuclei in the biopsy was defined as proliferative activity.

Statistical Analysis

Receiver operating characteristic curves were used to define optimum cutoff values for the prediction of histopathologic grade. Correlations between various ^{18}F-FDOPA uptake parameters and tumor proliferation (Ki-67 labeling index) were sought using linear regression analysis. Comparisons between groups were done using the Mann–Whitney *U* test. Statistical analysis was performed using SPSS software (version 16.0; SPSS Inc.) for Windows (Microsoft), and *P* values less than 0.05 were considered statistically significant.

RESULTS

Histopathology

The distribution of tumor types and grades is listed in Table 1. In brief, of the 59 lesions, 25 (42%) were classified as glioblastoma, 12 (20%) as astrocytoma, 11 (19%) as oligodendroglioma, 9 (15%) as oligoastrocytoma, and 2 (3%) as gliosarcoma. Thirteen of 59 lesions (22%) were classified as grade II, 19 (32%) as grade III, and 27 (46%) as grade IV (Fig. 1). No grade I lesions were identified in this patient population. The Ki-67 antibody staining index ranged from 1% to 90% in the 59 samples (mean ± SD, 22.2 ± 20.6), with 17.3% ± 15.9% in patients with newly diagnosed tumors and 25.2% ± 22.6% in recurrent brain tumors ($P = 0.20$). When stratified by tumor grades, the Ki-67 labeling index averaged 3.92 ± 2.36 in grade II, 17.68 ± 9.06 in grade III, and 34.26 ± 23.50 in grade IV lesions ($P < 0.0001$).

^{18}F-FDOPA Uptake and Tumor Grade

Correlation coefficients between tumor grade or Ki-67 and the different standardized uptake value (SUV) indices were nearly identical. Therefore, we elected to focus on reporting SUVmax, the most frequently used SUV parameter in the oncologic PET literature.

SUVmax averaged 2.44 ± 1.26 in grade II, 3.34 ± 1.02 in grade III, and 3.78 ± 1.48 in grade IV tumors (grade II vs. III, $P = 0.009$; grade II vs. IV, $P = 0.004$; Table 2). No significant differences in ^{18}F-FDOPA SUVmax were noted among grade III and IV tumors ($P = 0.42$).

When stratified into newly diagnosed and recurrent tumors, significant correlations between SUVmax and tumor grades were seen in newly diagnosed tumors but not recurrent tumors (Table 2; Fig. 2). In newly diagnosed tumors, SUVmax averaged 2.34 ± 1.35 in grade II, 3.38 ± 0.93 in grade III, and 5.19 ± 0.93 in grade IV tumors (grade II vs. III, $P = 0.044$; grade II vs. IV, $P = 0.007$; grade III vs. IV, $P = 0.010$). In recurrent tumors, SUVmax averaged 2.67 ± 1.18 in grade II, 3.33 ± 1.10 in grade III, and 3.38 ± 1.37 in grade IV tumors (grade II vs.

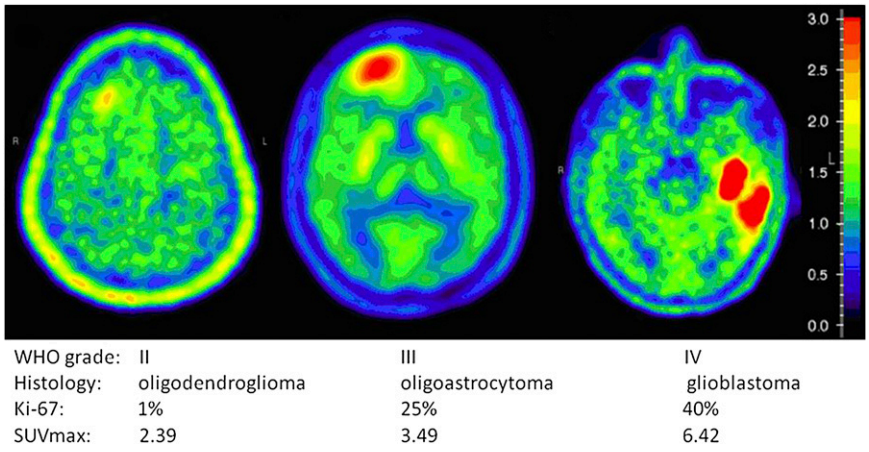

FIGURE 1. ^{18}F-FDOPA uptake in gliomas.

TABLE 2. ^{18}F-FDOPA Uptake in Various Tumors

Characteristic	All patients (n = 59)	Untreated (n = 22)	Pretreated (n = 37)
SUVmax ± SD	3.34 ± 1.38	3.45 ± 1.60	3.28 ± 1.26
Low grade			
WHO grade II	2.44 ± 1.26	2.34 ± 1.35	2.67 ± 1.18
WHO grade III	3.34 ± 1.02	3.38 ± 0.93	3.33 ± 1.10
WHO grade IV	3.78 ± 1.48	5.19 ± 0.93	3.38 ± 1.37
High grade	3.60 ± 1.32	4.22 ± 1.30	3.36 ± 1.26
WHO grade II vs. III	P = 0.009	P = 0.044	P = 0.33
WHO grade II vs. IV	P = 0.004	P = 0.007	P = 0.21
WHO grade III vs. IV	P = 0.42	P = 0.010	P = 0.76
WHO grade II vs. III/VI	P = 0.001	P = 0.005	P = 0.22
Mean Ki-67 index ± SD (%)	22.45 ± 20.69	17.32 ± 15.93	25.16 ± 22.59
WHO grade II	3.92 ± 2.36	3.44 ± 1.67	5.00 ± 3.56
WHO grade III	17.68 ± 9.06	19.29 ± 5.35	16.75 ± 10.78
WHO grade IV	35.19 ± 23.45	35.83 ± 16.25	33.81 ± 25.510

III, P = 0.38; grade II vs. IV, P = 0.23; grade III vs. IV, P = 0.78).

For clinical purposes and risk assessment, brain tumors are frequently stratified into high-grade and low-grade variants. Using this approach, significant differences between high-grade tumors and low-grade tumors were seen in newly diagnosed tumors but not recurrent tumors (P = 0.005 in newly diagnosed and P = 0.22 in recurrent tumors [Table 2]). Receiver-operating-characteristic curve analysis was used to identify the best ^{18}F-FDOPA SUVmax threshold between low- and high-grade tumors. For newly diagnosed tumors, an SUVmax threshold of 2.72 was the best discriminator for differentiating between high- and low-grade tumors (sensitivity and specificity of 85% and 89%, respectively; area under the curve, 0.86).

^{18}F-FDOPA Uptake and Tumor Proliferation

The correlations between the Ki-67 index and all SUV parameters were tested (Table 3). Most were significantly but only weakly correlated with the Ki-67 index (for SUVmax, r = 0.29, P = 0.027; Fig. 3A). The Ki-67 index and ^{18}F-FDOPA SUVmax in newly diagnosed tumors (n = 22; r = 0.66, P = 0.001; Fig. 3B) were significantly correlated. In contrast, no significant correlation was found between Ki-67 index and SUVmax in recurrent tumors (n = 37; r = 0.14, P = 0.41; Fig. 3C).

^{18}F-FDOPA SUVmax and Ki-67 index correlated in astrocytomas (n = 27; r = 0.51, P = 0.0007) but not in nonastrocytomas (n = 32; r = 0.09, P = 0.64). The correlation in astrocytomas was, again, significant only in newly diagnosed tumors (n = 12; r = 0.76, P = 0.004), not in recurrent tumors (n = 15; r = 0.39, P = 0.15).

DISCUSSION

In the current study, we analyzed differences in ^{18}F-FDOPA SUVs among grade II, III, and IV lesions (no grade I lesions were identified) in both newly diagnosed and recurrent gliomas. In addition, we explored whether the degree of ^{18}F-FDOPA uptake could provide information about tumor proliferative activity.

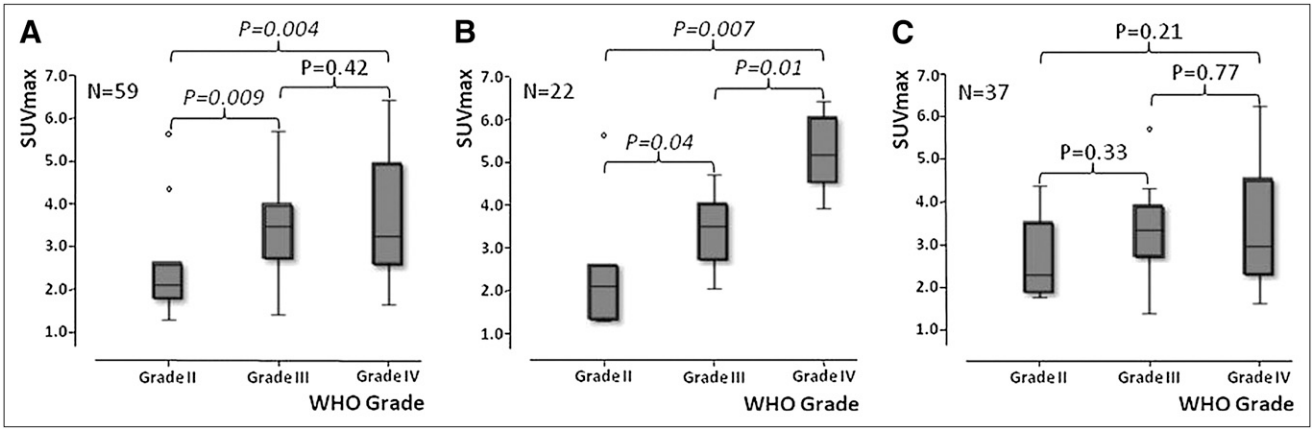

FIGURE 2. ^{18}F-FDOPA uptake and tumor grade in newly diagnosed and previously treated tumors combined (A), in newly diagnosed tumors (B), and in previously treated tumors (C).

TABLE 3. Linear Regression Results of Various SUV Indices and Ki-67 Index

Tumors	SUV index	*R*	*P*
All (*n* = 59)	Mean SUV	0.267	0.041
	SUVmax	0.289	0.027
	SUVmax20	0.310	0.017
	Tumor burden	0.364	0.005
	T/N mean SUV ratio	0.269	0.040
	T/N SUVmax ratio	0.284	0.029
	T/N SUVmax20 ratio	0.303	0.020
Newly diagnosed (*n* = 22)	Mean SUV	0.647	0.001
	SUVmax	0.656	0.001
	SUVmax20	0.660	0.001
	Tumor burden	0.666	0.001
	T/N mean SUV ratio	0.779	<0.0001
	T/N SUVmax ratio	0.778	<0.0001
	T/N SUVmax20 ratio	0.786	<0.0001
Treated (*n* = 37)	Mean SUV	0.113	0.51
	SUVmax	0.140	0.41
	SUVmax20	0.169	0.32
	Tumor burden	0.269	0.11
	T/N mean SUV ratio	0.024	0.89
	T/N SUVmax ratio	0.060	0.72
	T/N SUVmax20 ratio	0.085	0.62

SUVmax20 = mean values of voxels with top 20% SUVs; T/N ratio = ratio of ^{18}F-FDOPA uptake to mean values of contralateral normal brain.

Tumor burden was obtained by multiplying tumor volume and mean SUV in volume.

The current study demonstrated that in newly diagnosed tumors, an ^{18}F-FDOPA SUVmax of 2.72 discriminated between low- and high-grade tumors, with a sensitivity and specificity of 85% and 89%, respectively. Furthermore, ^{18}F-FDOPA uptake correlated significantly with the tumor cell proliferation by Ki-67 proliferation index.

Importantly, however, ^{18}F-FDOPA tumor uptake failed to provide reasonable predictions about tumor grade and proliferation in recurrent tumors that had undergone treatments. Thus, our study is consistent with previously published data. The studies that failed to show a correlation of ^{18}F-FDOPA uptake with tumor grade were performed in patient populations with mostly recurrent tumors, 13 of 19 (*22*) and 71 of 81, respectively (*23*), and another study that revealed differences between tumor grade and PET uptake used kinetic data in a group of 9 newly diagnosed tumors (*26*). Furthermore, previously reported studies that showed correlation between Ki-67 and tumor uptake of the amino acid tracer ^{11}C-methionine were performed in patients with newly diagnosed brain tumors (*14,18–20*).

The lack of correlation of ^{18}F-FDOPA uptake to tumor grade or proliferation index cannot be explained by a longer time between PET and histopathologic assessments, because this interval did not differ significantly between

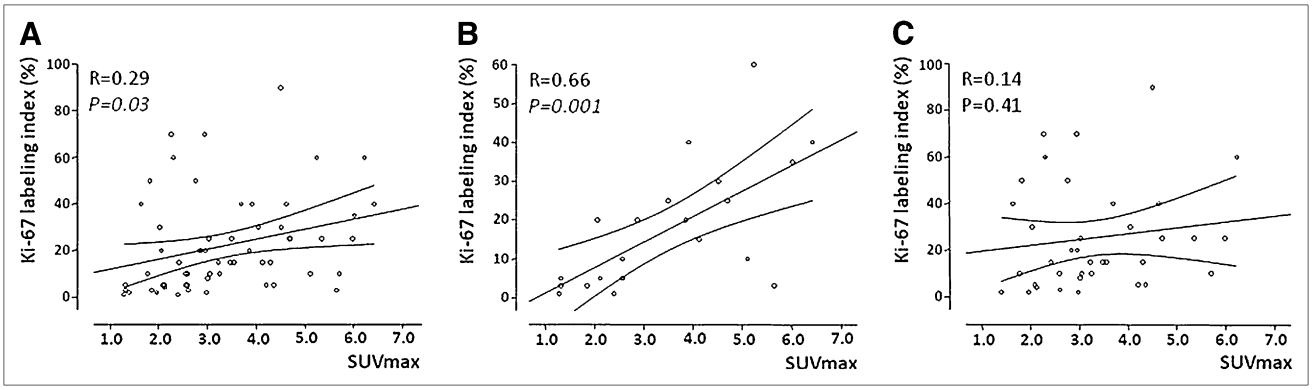

FIGURE 3. Correlation between ^{18}F-FDOPA uptake and Ki-67 index in newly diagnosed and previously treated tumors combined (A), in newly diagnosed tumors (B), and in previously treated tumors (C).

newly diagnosed (5.3 ± 3.9 wk) and recurrent tumors (4.0 ± 4.6 wk). We suspect that in recurrent tumors, blood–brain barrier breakdown contributes to the degree of ^{18}F-FDOPA uptake in addition to amino acid transport as described before (*37,38*). In our patient population of 37 patients with recurrent tumors, 32 had received chemotherapy or radiation before the PET study (86%). As recurrent tumors may have a wide range of blood–brain barrier breakdown, depending on previous treatments, it is not surprising that the correlation between ^{18}F-FDOPA PET uptake and tumor grade is better in those newly diagnosed tumors that have not gone through previous treatment.

The application of full kinetic modeling in ^{18}F-FDOPA PET studies of gliomas has been demonstrated to provide extra parameters to distinguish high- from low-grade recurrent tumors (*26*). Significant differences between high- and low-grade tumors were found for ^{18}F-FDOPA transport, influx rate, uptake (SUV), and distribution volume. Dynamic evaluation of *O*-(2-^{18}F-fluoroethyl)-L-tyrosine PET comprising absolute changes in peak SUV from frame to frame multiplied by the duration of the respective time frame has shown high diagnostic power in tumor grading in untreated and recurrent tumors (*11,39*). *O*-(2-^{18}F-fluoroethyl)-L-tyrosine PET also has the advantage over ^{18}F-FDOPA in that there is absence of uptake in the striatum.

It has been reported that tumor cells may upregulate amino acid transporter under adverse conditions (*40*). Our data further support ^{18}F-FDOPA as an amino acid analog in imaging gliomas because its uptake is predictive of tumor grade and proliferation potential. Thus, our study would predict that, in newly diagnosed gliomas, ^{18}F-FDOPA PET uptake may have significant prognostic value. Further study will demonstrate the value of ^{18}F-FDOPA PET uptake. The prognostic value of ^{18}F-FDOPA PET in recurrent tumors needs further study as well.

CONCLUSION

^{18}F-FDOPA PET of previously untreated gliomas provides potentially useful noninvasive predictions about tumor grade and proliferative activity. ^{18}F-FDOPA PET in previously treated gliomas does not provide information similar to that from untreated tumors. The prognostic value of ^{18}F-FDOPA PET awaits further study.

REFERENCES

1. McKeever PE, Ross DA, Strawderman MS, et al. A comparison of the predictive power for survival in gliomas provided by MIB-1, bromodeoxyuridine and proliferating cell nuclear antigen with histopathologic and clinical parameters. *J Neuropathol Exp Neurol.* 1997;56:798–805.
2. Wakimoto H, Aoyagi M, Nakayama T, et al. Prognostic significance of Ki-67 labeling indices obtained using MIB-1 monoclonal antibody in patients with supratentorial astrocytomas. *Cancer.* 1996;77:373–380.
3. Hoshino T, Ahn D, Prados MD, et al. Prognostic significance of the proliferative potential of intracranial gliomas measured by bromodeoxyuridine labeling. *Int J Cancer.* 1993;53:550–555.
4. Sallinen PK, Haapasalo HK, Visakorpi T, et al. Prognostication of astrocytoma patient survival by Ki-67 (MIB-1), PCNA, and S-phase fraction using archival paraffin-embedded samples. *J Pathol.* 1994;174:275–282.
5. Daumas-Duport C, Scheithauer BW, Kelly PJ. A histologic and cytologic method for the spatial definition of gliomas. *Mayo Clin Proc.* 1987;62:435–449.
6. Jager PL, Vaalburg W, Pruim J, et al. Radiolabeled amino acids: basic aspects and clinical applications in oncology. *J Nucl Med.* 2001;42:432–445.
7. Herholz K, Holzer T, Bauer B, et al. ^{11}C-methionine PET for differential diagnosis of low-grade gliomas. *Neurology.* 1998;50:1316–1322.
8. Laverman P, Boerman OC, Corstens FH, et al. Fluorinated amino acids for tumour imaging with positron emission tomography. *Eur J Nucl Med Mol Imaging.* 2002;29:681–690.
9. Bergstrom M, Collins VP, Ehrin E, et al. Discrepancies in brain tumor extent as shown by computed tomography and positron emission tomography using [^{68}Ga]EDTA, [^{11}C]glucose, and [^{11}C]methionine. *J Comput Assist Tomogr.* 1983;7:1062–1066.
10. Mosskin M, von Holst H, Bergstrom M, et al. Positron emission tomography with ^{11}C-methionine and computed tomography of intracranial tumours compared with histopathologic examination of multiple biopsies. *Acta Radiol.* 1987;28:673–681.
11. Pöpperl G, Kreth FW, Mehrkens JH, et al. FET PET for the evaluation of untreated gliomas: correlation of FET uptake and uptake kinetics with tumour grading. *Eur J Nucl Med Mol Imaging.* 2007;34:1933–1942.
12. Chung JK, Kim YK, Kim SK, et al. Usefulness of ^{11}C-methionine PET in the evaluation of brain lesions that are hypo- or isometabolic on ^{18}F-FDG PET. *Eur J Nucl Med Mol Imaging.* 2002;29:176–182.
13. Shields AF, Grierson JR, Dohmen BM, et al. Imaging proliferation in vivo with [F-18]FLT and positron emission tomography. *Nat Med.* 1998;4:1334–1336.
14. Hatakeyama T, Kawai N, Nishiyama Y, et al. ^{11}C-methionine (MET) and ^{18}F-fluorothymidine (FLT) PET in patients with newly diagnosed glioma. *Eur J Nucl Med Mol Imaging.* 2008;35:2009–2017.
15. Chen W, Cloughesy T, Kamdar N, et al. Imaging proliferation in brain tumors with ^{18}F-FLT PET: comparison with ^{18}F-FDG. *J Nucl Med.* 2005;46:945–952.
16. Jacobs AH, Thomas A, Kracht LW, et al. ^{18}F-fluoro-L-thymidine and ^{11}C-methylmethionine as markers of increased transport and proliferation in brain tumors. *J Nucl Med.* 2005;46:1948–1958.
17. Choi SJ, Kim JS, Kim JH, et al. [^{18}F]3′-deoxy-3′-fluorothymidine PET for the diagnosis and grading of brain tumors. *Eur J Nucl Med Mol Imaging.* 2005; 32:653–659.
18. Huang MC, Shih YH, Chen MH, et al. Malignancy of intracerebral lesions evaluated with ^{11}C-methionine-PET. *J Clin Neurosci.* 2005;12:775–780.
19. Sato N, Suzuki M, Kuwata N, et al. Evaluation of the malignancy of glioma using ^{11}C-methionine positron emission tomography and proliferating cell nuclear antigen staining. *Neurosurg Rev.* 1999;22:210–214.
20. Kim S, Chung JK, Im SH, et al. ^{11}C-methionine PET as a prognostic marker in patients with glioma: comparison with ^{18}F-FDG PET. *Eur J Nucl Med Mol Imaging.* 2005;32:52–59.
21. Heiss WD, Wienhard K, Wagner R, et al. ^{18}F-Dopa as an amino acid tracer to detect brain tumors. *J Nucl Med.* 1996;37:1180–1182.
22. Becherer A, Karanikas G, Szabo M, et al. Brain tumour imaging with PET: a comparison between [^{18}F]fluorodopa and [^{11}C]methionine. *Eur J Nucl Med Mol Imaging.* 2003;30:1561–1567.
23. Chen W, Silverman DH, Delaloye S, et al. ^{18}F-FDOPA PET imaging of brain tumors: comparison study with ^{18}F-FDG PET and evaluation of diagnostic accuracy. *J Nucl Med.* 2006;47:904–911.
24. Tripathi M, Sharma R, D'Souza M, et al. Comparative evaluation of F-18 FDOPA, F-18 FDG, and F-18 FLT-PET/CT for metabolic imaging of low grade gliomas. *Clin Nucl Med.* 2009;34:878–883.
25. Ledezma CJ, Chen W, Sai V, et al. ^{18}F-FDOPA PET/MRI fusion in patients with primary/recurrent gliomas: initial experience. *Eur J Radiol.* 2009;71:242–248.
26. Schiepers C, Chen W, Cloughesy T, et al. ^{18}F-FDOPA kinetics in brain tumors. *J Nucl Med.* 2007;48:1651–1661.
27. Brix G, Zaers J, Adam LE, et al. Performance evaluation of a whole-body PET scanner using the NEMA protocol. National Electrical Manufacturers Association. *J Nucl Med.* 1997;38:1614–1623.
28. Lartizien C, Comtat C, Kinahan PE, et al. Optimization of injected dose based on noise equivalent count rates for 2- and 3-dimensional whole-body PET. *J Nucl Med.* 2002;43:1268–1278.
29. Namavari M, Bishop A, Satyamurthy N, et al. Regioselective radiofluorodestannylation with [^{18}F]F2 and [^{18}F]CH3COOF: a high yield synthesis of 6-[^{18}F]Fluoro-L-dopa. *Int J Rad Appl Instrum [A].* 1992;43:989–996.
30. Bishop A, Satyamurthy N, Bida G, et al. Proton irradiation of [^{18}O]O_2: production of [^{18}F]F2 and [^{18}F]F2 + [^{18}F] OF2. *Nucl Med Biol.* 1996;23:189–199.
31. Bergstrom M, Litton J, Eriksson L, et al. Determination of object contour from projections for attenuation correction in cranial positron emission tomography. *J Comput Assist Tomogr.* 1982;6:365–372.
32. Kinahan PE, Townsend DW, Beyer T, et al. Attenuation correction for a combined 3D PET/CT scanner. *Med Phys.* 1998;25:2046–2053.

33. Nuyts J, Michel C, Dupont P. Maximum-likelihood expectation-maximization reconstruction of sinograms with arbitrary noise distribution using NEC-transformations. *IEEE Trans Med Imaging.* 2001;20:365–375.
34. Kleihues P, Cavenee WK, eds. *The WHO Classification of Tumors of the Nervous System*. 1st ed. Lyon, France: IARC Press; 2000.
35. Sarantopoulos GP, Gui D, Shintaku P, et al. Immunohistochemical analysis of lung carcinomas with pure or partial bronchioloalveolar differentiation. *Arch Pathol Lab Med.* 2004;128:406–414.
36. Terasaki H, Niki T, Matsuno Y, et al. Lung adenocarcinoma with mixed bronchioloalveolar and invasive components: clinicopathological features, subclassification by extent of invasive foci, and immunohistochemical characterization. *Am J Surg Pathol.* 2003;27:937–951.
37. Langen KJ, Muhlensiepen H, Holschbach M, et al. Transport mechanisms of 3-[^{123}I]iodo-α-methyl-L-tyrosine in a human glioma cell line: comparison with [^{3}H]methyl]-L-methionine. *J Nucl Med.* 2000;41:1250–1255.
38. Roelcke U, Radu EW, von Ammon K, et al. Alteration of blood-brain barrier in human brain tumors: comparison of [^{18}F]fluorodeoxyglucose, [^{11}C]methionine and rubidium-82 using PET. *J Neurol Sci.* 1995;132:20–27.
39. Po¨pperl G, Kreth GFW, Herms J, et al. Analysis of ^{18}F-FET PET for grading of recurrent gliomas: is evaluation of uptake kinetics superior to standard methods? *J Nucl Med.* 2006;47:393–403.
40. Sasajima T, Miyagawa T, Oku T, et al. Proliferation-dependent changes in amino acid transport and glucose metabolism in glioma cell lines. *Eur J Nucl Med Mol Imaging.* 2004;31:1244–1256.

JNM The Journal of NUCLEAR MEDICINE

Correlation of 6-^{18}F-Fluoro-l-Dopa PET Uptake with Proliferation and Tumor Grade in Newly Diagnosed and Recurrent Gliomas

Barbara J. Fueger, Johannes Czernin, Timothy Cloughesy, Daniel H. Silverman, Cheri L. Geist, Martin A. Walter, Christiaan Schiepers, Phioanh Nghiemphu, Albert Lai, Michael E. Phelps and Wei Chen

J Nucl Med. 2010;51:1532-1538.
Published online: September 16, 2010.
Doi: 10.2967/jnumed.110.078592

The Journal of Nuclear Medicine is published monthly.
SNMMI | Society of Nuclear Medicine and Molecular Imaging
1850 Samuel Morse Drive, Reston, VA 20190.
(Print ISSN: 0161-5505, Online ISSN: 2159-662X)

SNMMI SOCIETY OF NUCLEAR MEDICINE AND MOLECULAR IMAGING